Title

Low-Level Saturated Fatty Acid Palmitate Benefits Liver Cells by Boosting Mitochondrial Metabolism via CDK1-SIRT3-CPT2 Cascade.

Journal

Developmental cell, 52(2)

ISSN

1534-5807

Authors

Liu, Lin
Xie, Bowen
Fan, Ming
et al.

Publication Date

2020

DOI

10.1016/j.devcel.2019.11.012

Peer reviewed

Article

Developmental Cell

Low-Level Saturated Fatty Acid Palmitate Benefits Liver Cells by Boosting Mitochondrial Metabolism via CDK1-SIRT3-CPT2 Cascade

Graphical Abstract

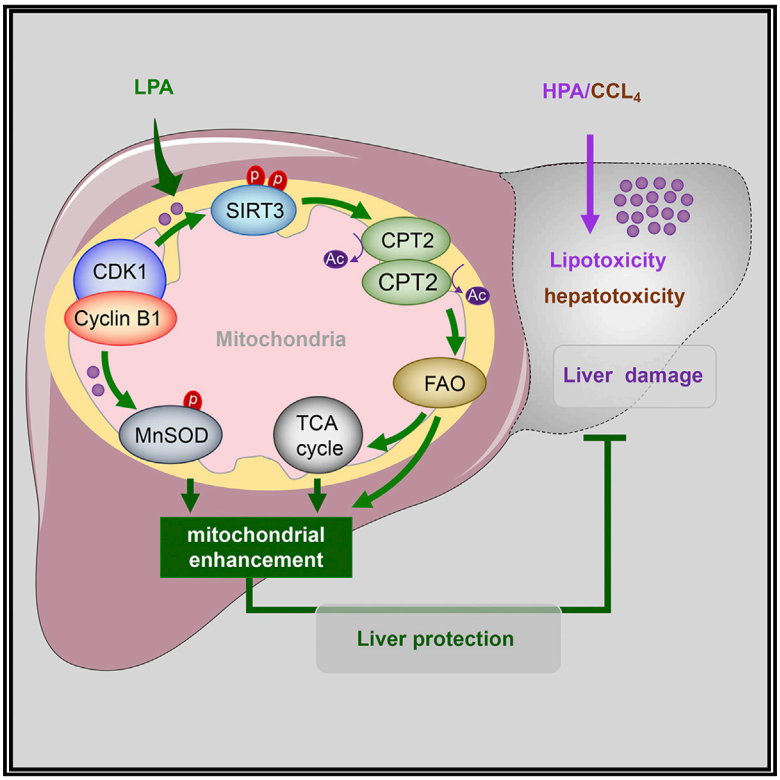

Authors

Lin Liu, Bowen Xie, Ming Fan, ..., Hong-Wu Chen, Yiyang Hu, Jian Jian Li

Correspondence

jijli@ucdavis.edu

In Brief

Liu et al. demonstrate that, whereas consumption of high-level palmitate (the major saturated fatty acid in the human diet) induced lipotoxic effects, consumption of low-level palmitate enhanced mitochondrial metabolism and compromised both high-level-palmitate-induced lipotoxicity and CCl_4-generated hepatotoxicity via a CDK1-SIRT3-CPT2 cascade.

Highlights

- Unlike high levels, low-level palmitate (LPA) enhances mitochondrial metabolism
- LPA-treated mice increase mitochondrial activity and alleviate CCl_4 hepatotoxicity
- LPA activates CDK1-SIRT3 pathway to enhance mitochondrial metabolism
- SIRT3 deacetylates and dimerizes CPT2 to augment fatty acid oxidation

Liu et al., 2020, Developmental Cell *52*, 1–14
January 27, 2020
https://doi.org/10.1016/j.devcel.2019.11.012

CellPress

Please cite this article in press as: Liu et al., Low-Level Saturated Fatty Acid Palmitate Benefits Liver Cells by Boosting Mitochondrial Metabolism via CDK1-SIRT3-CPT2 Cascade, Developmental Cell (2019), https://doi.org/10.1016/j.devcel.2019.11.012

Developmental Cell
Article

Low-Level Saturated Fatty Acid Palmitate Benefits Liver Cells by Boosting Mitochondrial Metabolism via CDK1-SIRT3-CPT2 Cascade

Lin Liu,[1,2,8] Bowen Xie,[1,8,9] Ming Fan,[1] Demet Candas-Green,[1] Joy X. Jiang,[3] Ryan Wei,[1,4] Yinsheng Wang,[5] Hong-Wu Chen,[6,7] Yiyang Hu,[2] and Jian Jian Li[1,7,10,*]

[1]Department of Radiation Oncology, School of Medicine, University of California, Davis, Sacramento, CA, USA
[2]Institute of Liver Diseases, Shuguan Hospital, Shanghai University of Traditional Chinese Medicine, Shanghai, China
[3]Department of Internal Medicine, Division of Gastroenterology and Hepatology, School of Medicine, University of California, Davis, Sacramento, CA, USA
[4]Lewis Katz School of Medicine, Temple University, Philadelphia, PA, USA
[5]Department of Chemistry, University of California, Riverside, Riverside, CA, USA
[6]Department of Biochemistry and Molecular Medicine, School of Medicine, University of California, Davis, Sacramento, CA, USA
[7]Comprehensive Cancer Center, University of California, Davis, Sacramento, CA, USA
[8]These authors contributed equally
[9]Present address: Xiangya Hospital, Central South University, Changsha, China
[10]Lead Contact
*Correspondence: jijli@ucdavis.edu
https://doi.org/10.1016/j.devcel.2019.11.012

SUMMARY

Saturated fatty acids (SFAs) (the "bad" fat), especially palmitate (PA), in the human diet are blamed for potential health risks such as obesity and cancer because of SFA-induced lipotoxicity. However, epidemiological results demonstrate a latent benefit of SFAs, and it remains elusive whether a certain low level of SFAs is physiologically essential for maintaining cell metabolic hemostasis. Here, we demonstrate that although high-level PA (HPA) indeed induces lipotoxic effects in liver cells, low-level PA (LPA) increases mitochondrial functions and alleviates the injuries induced by HPA or hepatoxic agent carbon tetrachloride (CCl_4). LPA treatment in mice enhanced liver mitochondrial activity and reduced CCl_4 hepatotoxicity with improved blood levels of aspartate aminotransferase (AST), alanine transaminase (ALT), and mitochondrial aspartate transaminase (m-AST). LPA-mediated mitochondrial homeostasis is regulated by CDK1-mediated SIRT3 phosphorylation, which in turn deacetylates and dimerizes CPT2 to enhance fatty acid oxidation. Thus, an advantageous effect is suggested by the consumption of LPA that augments mitochondrial metabolic homeostasis via CDK1-SIRT3-CPT2 cascade.

INTRODUCTION

Overconsumption of fat in the human diet, especially saturated fatty acids (SFAs) such as palmitate (PA), is associated with lipotoxicity-related disorders including obesity, cancer, cardiovascular diseases, diabetes, and nonalcoholic fatty liver diseases (NAFLD) (Forouhi et al., 2014; Mota et al., 2016; Xu et al., 2006). However, unreasonable limitations on SFA intake may be detrimental to normal cellular function, especially for mitochondrial integrity and metabolic homeostasis. Increasing evidence indicates that the connection between SFA consumption and SFA-induced health risks should be reconsidered based on epidemiological studies of energy-consumption-associated health menaces (Mancini et al., 2015; Willett et al., 2014). In fact, SFAs have been exonerated of blame for all-cause mortality in cardiovascular diseases, ischemic stroke, or type 2 diabetes (T2D) (de Souza et al., 2015; Lee et al., 2008). A recent study of 27,296 adults from 8 European countries, including 12,132 T2D cases, demonstrates a reduced incidence of T2D in people with increased intake of individual fatty acids (FAs) (Imamura et al., 2017). Based on these findings, it has been strongly suggested that SFA-associated cardiovascular risk should be reevaluated (Siri-Tarino et al., 2010), and a revision of global dietary guidelines has been suggested (Dehghan et al., 2017). The Practice Guideline Committee of the American Association for the Study of Liver has cautioned that polyunsaturated FAs may promote alcohol-induced liver disease whereas consumption of SFAs is potentially protective (O'Shea et al., 2010). A diet high in fat and low in carbohydrates, with exercise, has been recommended for reversing NAFLD (Noakes and Windt, 2017). A cluster of endogenous lipids with antidiabetic and anti-inflammatory functions is found to contain PA isomers including palmitic-acid-9-hydroxy-stearic-acid (Yore et al., 2014). Among other potential benefits, PA is known to increase membrane fluidity and glucose metabolism to inhibit hepatocellular carcinoma (Lin et al., 2017). These results, together with our epidemiological analysis on correlations of SFA-associated disease burden and motility (Table S1), suggest that although overconsumption of SFAs indeed causes lipotoxicity, consumption of a certain level of SFAs appears to be necessary for mitochondrial metabolism and normal cellular function.

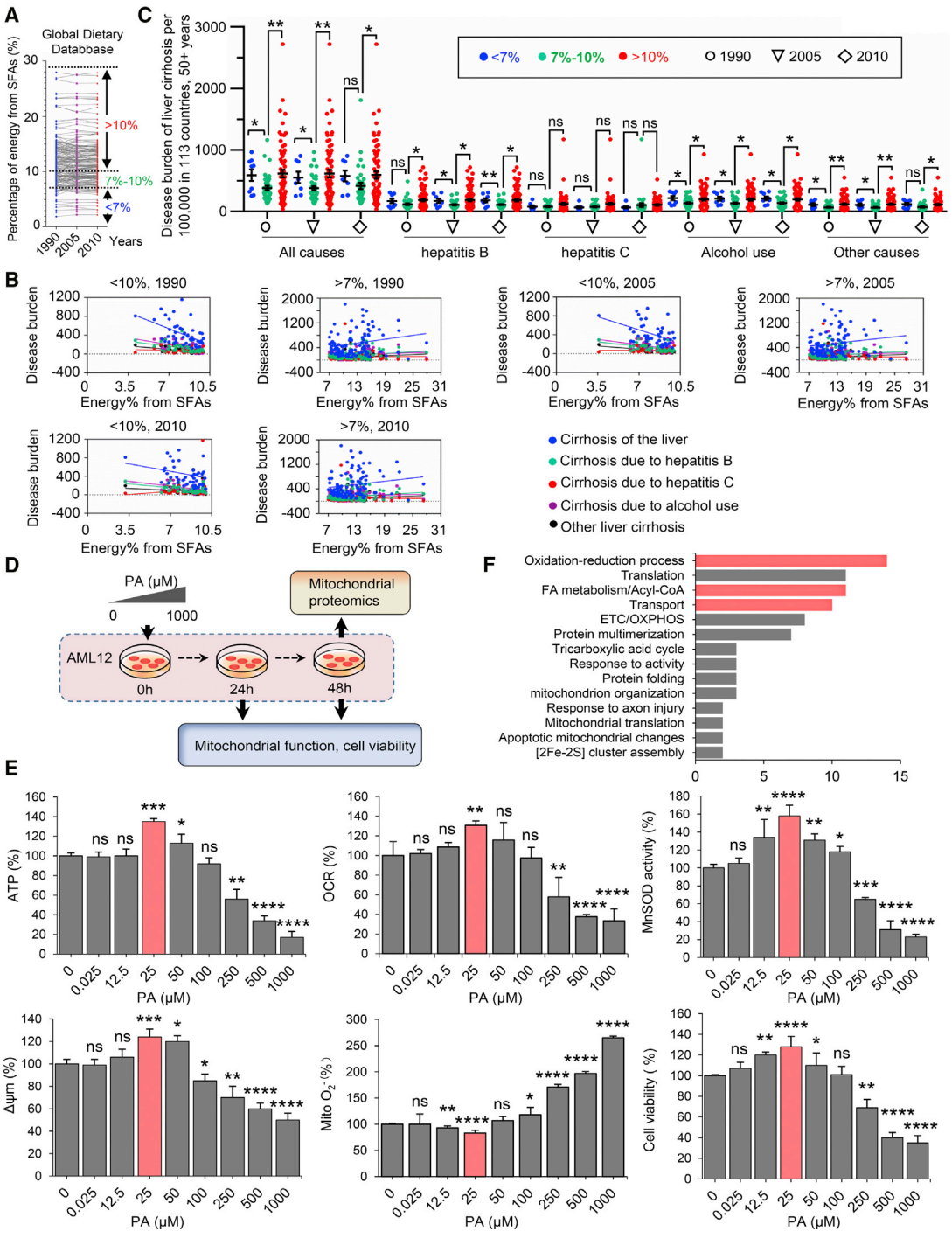

Figure 1. LPA Promotes Mitochondrial Homeostasis

(A) Status of SFA energy consumption in 113 countries in 1990, 2005, and 2010.

(B) Correlation of the burden of liver cirrhosis (defined as in [B]) related to alcohol use and all other pathogenic factors (hepatitis B and C and all other causes) with the percentage of energy derived from SFAs, based on the WHO's 2015 report on the Global Burden of Liver Cirrhosis (http://www.who.int/en) and Global Dietary Database (https://www.globaldietarydatabase.org/).

(C) The burden of all-cause liver cirrhosis is reduced by consumption of a certain range of SFAs (7%–10%) compared to either lower or higher consumption levels. Data points show the distribution of liver-cirrhosis-specific disability-adjusted life year (DALY) per 100,000 population aged 50 years and older in populations from 113 countries (mean ± SEM, *$p < 0.05$; **$p < 0.01$; ns, no significance).

(D) Schematic of the experiments characterizing the mitochondrial function and cell viability of mouse liver AML12 cells treated with a PA concentration gradient.

(legend continued on next page)

The metabolic homeostasis in mitochondria is essential for human health requiring efficient energy dynamics for carrying out the fundamental cellular functions (Berardi and Chou, 2014; Grazier et al., 2009; Senyilmaz et al., 2015). However, lipotoxicity-induced accumulation of PA especially in non-adipose cells could be a result of experimentally impairing mitochondrial oxidative capacity (Geng et al., 2015; Leamy et al., 2014). Such PA-mediated lipotoxic effects are usually generated by a range of high PA concentrations applied in both *in vitro* and *in vivo* study models (Table S2). Thus, although such HPA models have generated relevant information to mimic clinical lipotoxic effects, they may cause us to overlook a potential advantageous function of a physiological level of PA that is required in the evaluation of SFA-associated health issues. PA is the first product during FA synthesis and the major precursor for the generation of long-chain FAs, which are required for many fundamental cellular functions, such as palmitoylation to enhance the hydrophobicity and determine the localization of proteins (Linder and Deschenes, 2007). Therefore, defining a physiological level of PA required for maintaining mitochondrial homeostasis in non-adipose cells especially in liver will provide critical information for optimizing a well-balanced energy intake to prevent lipotoxicity-associated diseases.

SIRT3, primary mitochondrial deacetylase, plays a critical role in maintaining mitochondrial metabolic homeostasis via deacetylation of mitochondrial proteins (Qiu et al., 2010; Wang et al., 2019; Winnik et al., 2015; Yang et al., 2016). An array of key mitochondrial metabolic factors are under the SIRT3 regulation, including complex I (Brenmoehl and Hoeflich, 2013), manganese superoxide dismutase (MnSOD) (Tao et al., 2010), and isocitrate dehydrogenase 2 (Yu et al., 2012). Recently, a MnSOD-K68 acetylation mimic mutant that blocks SIRT3-mediated deacetylation is linked with procarcinogenesis (Zhu et al., 2019). SIRT3-mediated mitochondrial homeostasis is achieved via preserving the balance between bioenergetic output and clearance of the reactive oxygen species (ROS) (Ozden et al., 2011; Yu et al., 2012). FAs are transferred from the cytoplasm into the mitochondrial matrix by the carnitine O-palmitoyltransferases CPT1 and 2 (Corbet et al., 2016) for the synthesis of ketone bodies through fatty acid oxidation (FAO) and the trichloroacetic acid (TCA) cycle. SIRT3 is shown to regulate the activity of long-chain acyl coenzyme A dehydrogenase (LCAD) in FAO (Hirschey et al., 2010) and is required for ameliorating hepatic lipotoxicity (Bao et al., 2010). In addition, CDK1 activates SIRT3 (Liu et al., 2015) and regulates mitochondrial protein influx and bioenergetics (Harbauer et al., 2014; Wang et al., 2014). These findings contribute to the hypothesis that the CDK1-SIRT3-FAO pathway could be essential for the potential metabolic benefits induced by consumption of a low level of SFAs. This study reveals an advantageous mitochondrial homeostasis in low-level PA (LPA)-treated mouse liver cells with CRISPR-edited gene deficiency and *in vivo* mouse hepatotoxicity. LPA boosts mitochondrial metabolism and enhances the capacity to defend lipotoxicity in liver cells or carbon tetrachloride (CCl_4)-induced mouse hepatotoxicity. SIRT3 is activated by CDK1-mediated phosphorylation in mitochondria followed by SIRT3-mediated deacetylation and dimerization of CPT2. Thus, LPA generates a favorable effect in liver cells via the CDK1-SIRT3-CPT2 cascade.

RESULTS

LPA Promotes Mitochondrial Homeostasis and Limits Hepatotoxic Injury

Referring to the World Health Organization (WHO) recommendation and study-based suggestion (Dehghan et al., 2017) for a standard SFA consumption level (7%–10%, marked green in Figure 1A), we used the Global Dietary Database (https://www.globaldietarydatabase.org/) to estimate the correlation between consumption level of SFAs and the disease burden of liver cirrhosis (Figures 1B and 1C) as well as the mortality from other lipotoxicity-related diseases (Figure S1). The burden of liver cirrhosis from all causes (alcohol use, pathogenic factors, hepatitis B and C, and all other causes) was reduced in populations with SFA energy intake between 7% and 10% compared to populations with SFA intake of either >10% or <7% (Figures 1B and 1C; Table S1). The mortality of major lipotoxicity-related disease was indeed increased with the level of SFA-based energy intake >10%; however, no difference in mortality was detected in populations with SFA consumption of 7%–10% and <7% (Figure S1). Referring to HPA being used to induce lipotoxicity to mimic clinical observations of SFA overconsumption, cellular response to the increased PA ($\geq$100 μM) and lowered PA (<100 μM) concentrations as well as animal tests on the liver response to a PA-enriched high-fat diet (HFD) were summarized in Table S2, which was used to estimate the HPA and LPA concentrations in this study.

Regarding the lipotoxicity-associated major human diseases and mortality, our epidemiological analyses revealed a potential undiscovered benefit by consumption of a certain low level of SFA. We thus assumed that consumption of PA at a certain low level may benefit cellular metabolism especially in non-adipose cells such as liver cells that play the fundamental roles in lipid metabolism. Following this line of reasoning, we investigated mitochondrial function and cell viability in mouse liver AML12 cells exposed to a gradient of PA concentrations (0–1,000 μM) for 24 h and 48 h (Figure 1D). Indeed, HPA-induced lipotoxicity was recapitulated with reduced mitochondrial functions including ATP generation, oxygen consumption rate (OCR), MnSOD activity, membrane potential ($\Delta\psi m$), and cell viability treated with HPA (>250 μM), and mitochondrial O_2^- increased proportionally with PA concentration (Figure 1E). In contrast, no detectable mitochondrial dysfunction was observed in cells

(E) Mitochondrial activities including ATP generation, OCR, MnSOD activity, $\Delta\psi m$, O_2^-, and cell viability were measured in AML12 cells treated with PA at the indicated concentration for 48 h. Data were presented as the percentage of the control after normalization to the samples with BSA 0.05%. n = 3, mean ± SEM, *p < 0.05; **p < 0.01, ***p < 0.001, ****p < 0.0001 versus BSA; ns, no significance. LPA treatment for 24 h is shown in Figure S2A.

(F) Mitochondrial proteomics of AML12 cells measured 48 h after LPA (25 μM) treatment versus cells treated with 0.05% BSA. Data were categorized by DAVID bioinformatics, proteins in FA metabolism and redox balance were marked in red.

See also Figures S1–S3.

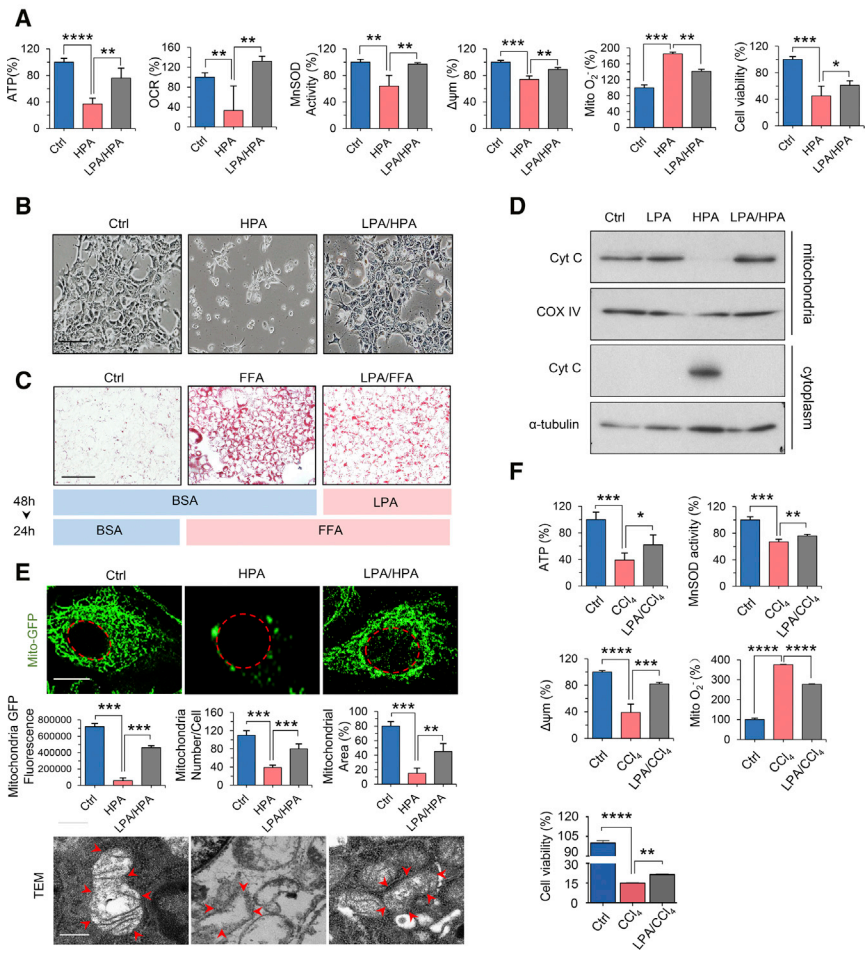

Figure 2. LPA Pre-exposure Prevents Mitochondrial Injury Induced by HPA or CCl_4

(A) Mitochondrial ATP, OCR, MnSOD activity, $\Delta\psi m$, O_2^-, and cell viability measured in AML12 cells pretreated with BSA or LPA for 48 h, followed by HPA (500 μM) for 24 h n = 3, mean ± SEM, *p < 0.05, **p < 0.01, ***p < 0.001, ****p < 0.0001 versus HPA.

(B) Morphological alterations of AML12 cells treated with BSA (Ctrl), HPA, or HPA plus pretreatment with LPA. Scale bar, 100 μm.

(C) Oil red O staining of AML12 cells pretreated with BSA (Ctrl) or LPA for 48 h followed by BSA or free fatty acids (FFAs) (oleic acid [OA]:PA = 2:1) for 24 h. Scale bar, 100 μm.

(D) Western blotting of mitochondrial or cytoplasmic proteins of AML12 cells treated in (A). Cyt C, cytochrome C; COX IV, mitochondrial loading control.

(E) Mass and integrity analysis of mitochondria of AML12 cells treated as in (A). Upper panel, fluorescence microscopy images of GFP-labeled mitochondria (Mito-GFP; nuclear membrane is indicated with a dashed red line). Quantification of mitochondrial mass with ImageJ; n = 30, mean ± SEM versus HPA, **p < 0.01, ***p < 0.001 (scale bar, 4 μm). Lower panel, transmission electron microscopic (TEM) images of mitochondrial ultrastructure (mitochondrial membrane is indicated with red arrows [scale bar, 500 nm]).

(F) Mitochondrial function and cell viability were measured in AML12 cells treated with LPA followed by CCl_4 exposure (10 μM) for 3 h. n = 3, mean ± SEM, *p < 0.05, **p < 0.01, ***p < 0.001, ****p < 0.0001 versus CCL_4.

See also Figure S4.

treated with <100 μM PA. Surprisingly, ATP, OCR, MnSOD activity, and $\Delta\psi m$ were enhanced by 35%, 30%, 58%, and 24%, respectively, with a corresponding reduction in mitochondrial O_2^- and increased cell viability, in cells treated with 25 μM PA (this PA concentration was determined as the LPA for liver cells; Figures 1E and S2A). Similarly, the LPA-boosted mitochondrial functions were also observed in primary cultured mouse liver cells (Figure S2B). In addition, liquid chromatography mass spectrometry (LC/MS)-based proteomic analysis of LPA-treated AML12 cells further revealed about 170 proteins involved in LPA-induced reprogramming of mitochondrial metabolism and homeostasis (Figure 1F). These proteins were involved in FAO, redox metabolism, and oxidative phosphorylation (OXPHOS) (Figures 1F and S3) that appeared to be different from the key pathways induced *in vivo* response following a diet with high calories from fat (Table S3), supporting a potential LPA benefit via a unique signaling pathway.

LPA Alleviates Mitochondrial Injury Induced by HPA

We then wondered if such LPA-enhanced mitochondrial activity could be defensive against the lipotoxic effects induced by overconsumption of SFAs. AML12 cells and primary mouse liver cells were pretreated with LPA for 48 h and then challenged with a dose of HPA (500 μM). Surprisingly, the entire index of mitochondrial functions tested was improved by LPA with reduced O_2^- levels and increased cell viability (Figures 2A and S4A). However, the boosted levels of mitochondrial activity appeared to be time dependent. LPA pretreatment for 24 h did not enhance MnSOD activity, cell viability, and FAO, although ATP generation, OCR, $\Delta\psi m$, and O_2^- levels were improved (Figures S4B and S4C). Consistently, accumulated free fatty acids (FFAs) and severe cellular damage were detected in cells treated with HPA, whereas LPA pretreatment prevented such changes (Figure 2B) and reduced FFAs (Figure 2C), suggesting that LPA-pretreated liver cells are able to attenuate lipid accumulation with an increased FAO capacity. LPA was also shown to prevent HPA-induced cytochrome C release from mitochondria (Figure 2D), with well-maintained mitochondrial mass, number, and structural integrity compared with the cells treated with HPA alone (Figure 2E).

LPA Reduces Mitochondrial Injury and Alleviates Hepatotoxicity Induced by CCl_4

We next asked whether LPA-enhanced mitochondrial function could also be protective against ROS-mediated mitochondrial injury and hepatotoxicity. Mitochondrial function and cell viability were measured in AML12 cells with or without LPA pretreatment following exposure to CCl_4, a well-studied toxic agent that

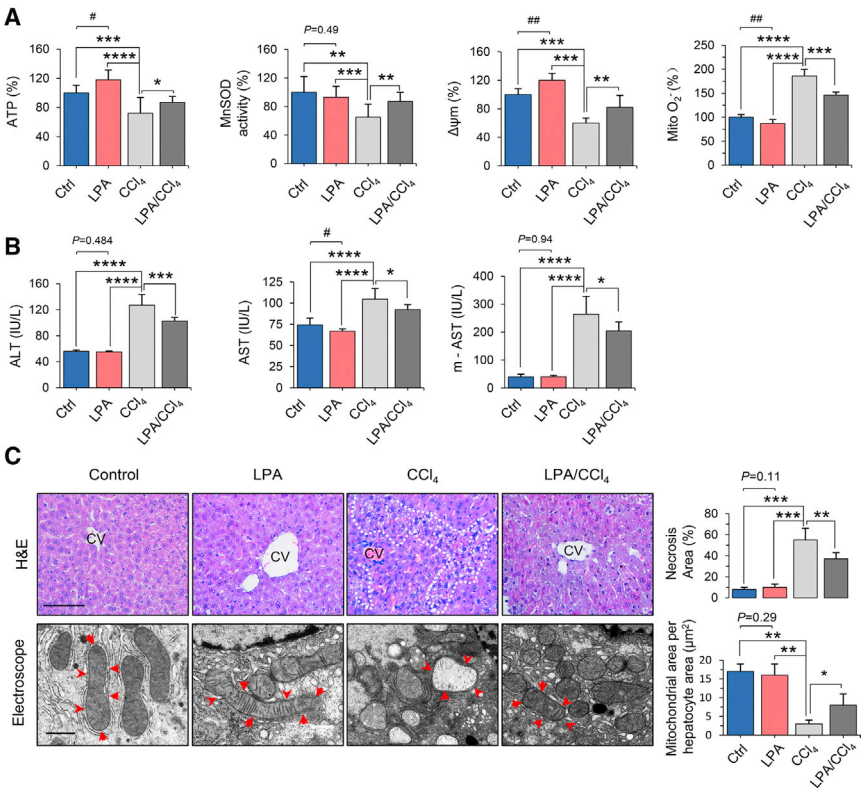

Figure 3. LPA Boosts Mitochondrial Activity and Reduces CCl_4-Induced Liver Injury

(A) Mitochondrial functions of primary liver cells isolated from control and LPA-, CCl_4-, and LPA/CCl_4-treated mice. n = 8, mean ± SEM, *p < 0.05, **p < 0.01, ***p < 0.001, ****p < 0.0001, versus CCL_4; #p < 0.05, ##p < 0.01 versus Ctrl.

(B) Blood levels of AST, ALT, and mitochondrial AST (m-AST) in the animals of control, LPA, CCl_4, and LPA and CCl_4 groups. n = 8, mean ± SEM, *p < 0.05, ***p < 0.001, ****p < 0.0001 versus CCL_4, #p < 0.05 versus Ctrl.

(C) Images of CCl_4-induced inflammatory infiltration and necrotic lesions in liver tissue (H&E staining and quantification, top) and mitochondrial damage (TEM, bottom) in livers from mice from the control, LPA, CCl_4, and LPA/CCl_4 groups. The necrotic lesions in H&E staining were analyzed with ImageJ software, and the mitochondrial structural integrity was scored by mitochondrial area per hepatocyte, μm^2. Top scale bar, 40 μm; bottom scale bar, 500 nm. n = 8, mean ± SEM, *p < 0.05; **p < 0.01, ***p < 0.001 versus CCL_4.

See also Figure S5.

impairs mitochondrial function via ROS generation (Domenicali et al., 2009). As expected, exposure to CCl_4 decreased ATP generation, MnSOD activity, Δψm, and cell viability and elevated levels of mitochondrial O_2^-; however, all of these changes were significantly ameliorated in cells pretreated with LPA (Figure 2F). Using GFP-labeled mitochondrial proteins and transmission electron microscopy, we showed that mitochondrial mass and ultrastructural integrity were markedly protected in LPA-pretreated cells compared to the control cells without LPA pretreatment (Figure S4D).

LPA-mediated hepatoprotective function was then tested using the established mouse model of CCl_4-induced acute liver injury (Morales-Garza et al., 2017). The most effective *in vivo* PA concentration was determined based on tests in mice showing that intragastric gavage with 0.5 mg/mL of PA, but not 5.0 mg/mL or 100 mg/mL, increased mitochondrial Δψm and reduced O_2^- in the liver (Figure S5A). Thus, 0.5 mg/mL PA was applied as the *in vivo* LPA. The optimized concentration of CCl_4 was also established by exposure of mice to 100%, 50%, and 10% solutions of CCl_4 (Figures S5B and S5C). The grade of hepatotoxicity and mitochondrial injury were then assessed in mice pretreated by intragastric gavage with 0.5 mg/mL PA for 3, 6, and 12 days, followed by treatment with 100% CCl_4 (Figure S5G). Remarkably, mice receiving the pretreatment of LPA for 12 days significantly reduced the degree of mitochondrial damage induced by CCl_4 measured by ATP generation, MnSOD activity, Δψm, and mitochondrial O_2^- (Figure 3A). The mice showed no significant alterations in blood levels of alanine transaminase (ALT) and mitochondrial aspartate transaminase (m-AST) in response to *in vivo* LPA treatment, though aspartate aminotransferase (AST) was slightly lowered (Figure 3B). However, the rise in blood levels of ALT, AST, and m-AST triggered by CCl_4 (127%, 41%, and 553%, respectively) was markedly lowered in LPA-pretreated mice (Figure 3B). No obvious alterations in body weight and liver weight were observed in any group of mice (Figures S5D and S5E). LPA-mediated liver protection was further demonstrated by the inhibition of inflammatory infiltration in the CV (central veins) area in the liver tissues (Figure 3C, top) and well-preserved mitochondrial structure and cristae (Figure 3C, bottom). In addition, no PA accumulation was detected in the livers of LPA-pretreated mice (Figure S5F). Interestingly, mice with LPA administration for 3 and 6 days did not show noticeable LPA-mediated protection against CCl_4-mediated hepatotoxicity and metabolic damage (Figures S5H and S5I). Together with the *in vitro* data showing less protection by LPA pretreatment at 24 versus 48 h (Figure S4B), these results indicate that a lag time is required for LPA to induce mitochondrial protection. In mice, a period of 12 days of LPA administration seems to be required to provide a protective effect.

CDK1 Boosts SIRT3 Activity in LPA-Induced Reprogramming of Mitochondrial Metabolism

We and others have previously reported that CDK1 functions as a sensor for cellular energy demand and mitochondrial bioenergetics (Harbauer et al., 2014; Qin et al., 2015; Wang et al., 2014). Here, we found that cyclin B1, the partner of CDK1 for CDK1 activation, and the activated form of CDK1 (phosphorylated at T161; pCDK1-T161) were increased in the mitochondria of cells treated with LPA for 48 h but decreased in the mitochondria of cells incubated with HPA (Figures 4A and S6A). To determine

whether CDK1-mediated mitochondrial energy sensing is involved in LPA-promoted mitochondrial homeostasis, mitochondria-directed wild-type (WT) CDK1 and kinase-deficient CDK1 were separately transfected into AML12 cells (Figure S6B). Expression of mitochondria-directed WT CDK1 but not the kinase-deficient mutant enhanced mitochondrial function and cell viability (Figures 4B and S6C). In CCl_4 hepatotoxic tests (Figure 4C), surprisingly, pCDK1-T161 was totally abolished in the liver mitochondria of mice treated with CCl_4 alone, but a substantial amount of pCDK1-T161 and cyclin B1 were preserved in the liver mitochondria of mice pretreated with LPA for 12 days before CCl_4 administration (Figure 4D).

Mitochondrial homeostasis is linked to the regulation of SIRT3, a well-defined mitochondrial deacetylase (Kim et al., 2010; Tao et al., 2010) that attenuates PA-induced ROS (Koyama et al., 2011). SIRT3 activity can be upregulated by CDK1 by irradiation (Liu et al., 2015). As expected, mitochondrial ATP production and OCR were enhanced 50% and 56%, respectively, in AML12 cells harboring WT SIRT3 and reduced 33% and 91%, respectively, in cells expressing the mutant of SIRT3-T8A/S17A (Figure 4E). Information on the SIRT3 double mutant and other mitochondrial functions including $\Delta\psi m$, O_2^- and cell viability were shown in Figure S6F. A direct interaction between CDK1 and SIRT3 was detected in AML12 cells and was remarkably boosted by LPA treatment (Figure 4F). To determine whether the SIRT3 phosphorylation is also enhanced by LPA, immunoprecipitation (IP) was conducted first with an anti-phospho-S and T antibody, followed by immunoblotting with anti-SIRT3 antibody, demonstrating that phosphorylated SIRT3 was noticeably elevated by LPA pretreatment for both 24 and 48 h. At the same time, the acetylation level of mitochondrial proteins was reduced by 24 and 48 h LPA incubation, confirming that incubation of AML12 cells with LPA activates SIRT3 (Figure 4G). This result again supports the pattern of time-dependent LPA-mediated mitochondrial homeostasis.

In vivo tests also demonstrated a striking enhancement of CDK1-SIRT3 complex formation (Figure 4H) and a remarkable elevation of phosphorylated SIRT3 (Figure 4I) in mice pretreated with LPA for 12 days. Levels of pCDK1-T161 and acetylated mitochondrial proteins showed a dependence on the duration of the pretreatment with LPA, with the greatest difference at 12 days (Figure 4J). Although reduced acetylation of mitochondrial proteins and enhanced pCDK1-T161 were observed in the livers of mice treated with LPA for 3 and 6 days (Figure 4J), recall that no detectable improvement in blood levels of ALT and AST were observed at these time points (Figures S5G and S5H), indicating that a lag period is required for full enhancement of liver mitochondrial function via LPA-mediated SIRT3 activation. Together, these results clearly demonstrate that LPA can promote adaptive mitochondrial metabolism and homeostasis via CDK1-mediated SIRT3 activation.

CPT2 Is Deacetylated and Activated Following CDK1-SIRT3 Activation

Following the finding of LPA-mediated activation of the CDK1-SIRT3 pathway, we then determined the potential key enzymes in mitochondrial FAO. SIRT3 is shown to regulate mitochondrial FAO (Hirschey et al., 2010) and required for ameliorating hepatic lipotoxicity (Bao et al., 2010). CPT2 has been indented to be a critical FAO enzyme located on the inner mitochondrial membrane (Figure S6G) (Hsiao et al., 2006). Although CPT2 was not in the list of the LPA-enhanced profile by proteomics analysis (Figures 1F and S3A), and the protein level was not enhanced (Figure 5A), LPA increased the CPT2 enzymatic activity by 60% when measured by a ^{14}C-radiochemical assay. Referencing the reported SIRT3-mediated deacetylation residues (Tao et al., 2010; Zhu et al., 2019), two potential deacetylation candidate residues lysine 453 and 457 (K453 and 457) in CPT2 were predicted by SWISS-MODEL (Figures S6G–S6I). Direct interaction of SIRT3 and CPT2 was detected and strikingly enhanced by LPA (Figure 5B), and the acetylated form of CPT2 was also reduced (Figure 5B). Furthermore, this result was recapitulated in mouse liver pretreated with LPA (Figure 5C). Thus, both *in vitro* and *in vivo* results demonstrate that SIRT3-mediated CPT2 deacetylation is involved in LPA-induced mitochondrial metabolism.

To verify that SIRT3 is specifically phosphorylated by CDK1 in LPA-mediated mitochondrial enhancement, we constructed lentiviral vectors expressing WT murine SIRT3, mutant SIRT3-T8A, mutant SIRT3-S17A, and double mutant SIRT3-T8A/S17A in AML12 cells (Figures 5D, S6D, and S6E). Interestingly, compared to cells expressing WT SIRT3, the acetylated CPT2 was not enhanced in cells expressing SIRT3-T8A, but cells harboring the SIRT3-S17A or SIRT3-T8A/S17A constructs showed increased CPT2 acetylation (Figure 5D), indicating that S17 of SIRT3 is specifically required for SIRT3-mediated CPT2 deacetylation.

Again, to determine whether the phosphorylation of SIRT3 at S17 is critical for CPT2 activation, CRISPR/Cas9-edited SIRT3 knockout cells (SIRT3-KO; clone CRISPR#1, Figure 5E; targeting sequences shown in Table S4) were reconstituted with WT SIRT3 or SIRT3-S17A, showing that the SIRT3 mutation at S17 (S to A) significantly increased the acetylation of CPT2 (Figure 5F), indicating that S17 is required for SIRT3-mediated CPT2 deacetylation. Moreover, CPT2 activity, which decreased by 59% in SIRT3-KO cells, was completely rescued (104%) by re-expressing WT SIRT3. In contrast, the rescuing capacity was severely hampered in cells transfected with the SIRT3-S17A or SIRT3-T8A/S17A mutants (Figure 5G).

SIRT3-Mediated CPT2 Dimerization Is Required for LPA-Enhanced FAO

CPT1A is a carnitine-acylcarnitine translocase locating within the mitochondrial outer membrane. It self-assembles into an oligomeric complex and catalyzes the rate-limiting step in the transport of long-chain acyl-CoAs. CPT1A and CPT2 share 50% homology. We thus speculated that CPT2 functions as an oligomer enhanced by SIRT3-mediated deacetylation. Importantly, two potential acetylation sites K453 and K457 were located (Figure S6G) with p values of 0.0009 and 0.0299, respectively, (http://bioinfo.bjmu.edu.cn/huac/predict_p/) and highly conserved across species (Figure S6H). To test whether K453 and K457 are required for the dimerization of CPT2, AML12 cells were transfected with a lentivirus expressing v5-tag-linked CPT2, and as expected, via native gel analysis, a band close to twice the expected size of CPT2 (68 kDa) was detected in control cells and remarkably enhanced by LPA pretreatment (Figure 6A). The role of deacetylation of K453 and K457 was then

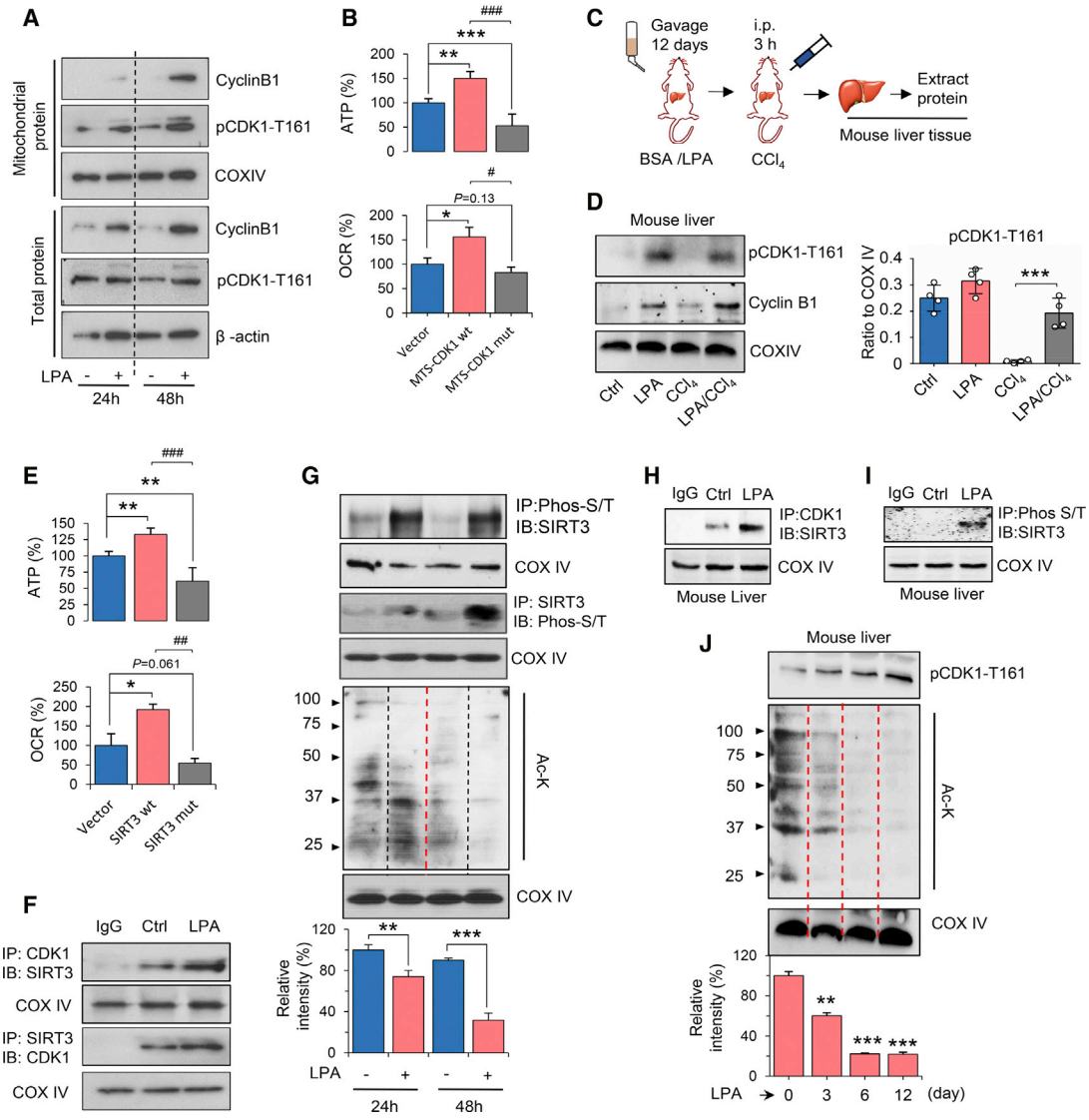

Figure 4. LPA Enhances Mitochondrial Homeostasis via CDK1-Mediated SIRT3 Activation

(A) Total and mitochondrial cyclin B1 and activated CDK1 (pCDK1-T161) in AML12 cells treated with LPA for 24 and 48 h.

(B) ATP and OCR measured in AML12 cells transfected with the mitochondria-targeted wild-type (WT) or kinase-deficient (mut) CDK1. n = 3, mean ± SEM, *p < 0.05, **p < 0.01, ***p < 0.001 versus vector; $^{\#}$p < 0.05, $^{\#\#\#}$p < 0.001 versus MTS-CDK1 wt.

(C) Experimental design for detecting the CDK1-SIRT3 pathway in mouse livers treated with LPA. The procedures for LPA gavage, CCl_4 injury, and mitochondrial preparation from mouse livers were the same as in Figure S5A.

(D) Western blotting of mitochondrial cyclin B1 and pCDK1-T161 from pooled liver tissues of mice in the control, LPA, CCl_4, and LPA/CCl_4 groups. Right, relative levels of pCDK1-T161 were quantified by ImageJ. n = 4, mean ± SEM. ***p < 0.001.

(E) ATP and OCR of AML12 cells transfected with WT or double mutant SIRT3-T8A/S17A. n = 3, mean ± SEM, *p < 0.05, **p < 0.01 versus vector. $^{\#\#}$p < 0.01, $^{\#\#\#}$p < 0.001 versus SIRT3 WT.

(F) Enhanced interaction between CDK1 and SIRT3 was detected by immunoprecipitation (IP) in mitochondrial fractions of LPA-treated AML12 cells. IB, immunoblot.

(G) Phosphorylated SIRT3 and acetylated proteins of mitochondrial fractions were detected in AML12 cells treated with or without LPA. Acetylated mitochondrial proteins were quantified by ImageJ. n = 4, mean ± SEM, **p < 0.01, ***p < 0.001.

(H) Interaction between CDK1 and SIRT3 in liver tissues of control and LPA-treated mice.

(I) Phosphorylated SIRT3 proteins detected in liver mitochondria of LPA-treated mice.

(J) pCDK1-T161 and acetylated proteins in liver mitochondria of mice treated with LPA for 0, 3, 6, and 12 days. Acetylated mitochondrial proteins were quantified by ImageJ. n = 4, mean ± SEM, **p < 0.01, ***p < 0.001 versus day 0.

See also Figure S6.

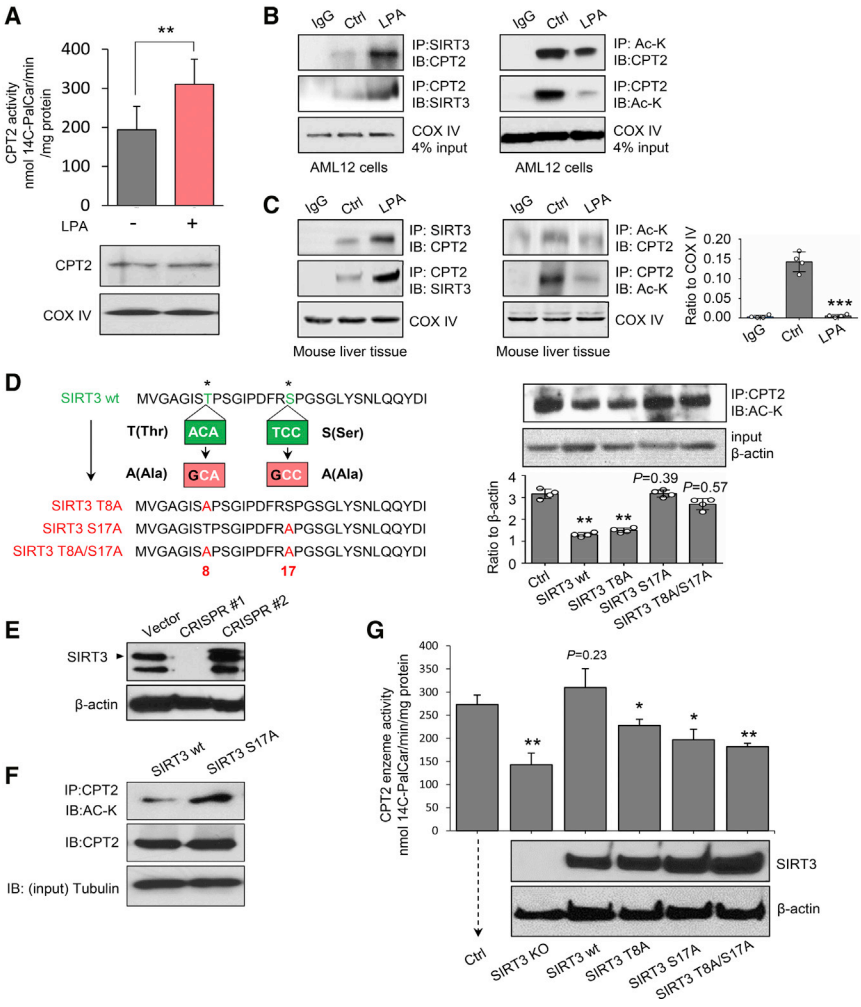

Figure 5. SIRT3 S17 Phosphorylation Is Required for Deacetylation and Activation of CPT2

(A) Enzymatic activity was measured by radiochemical assay in LPA-treated AML12 cells. n = 3, mean ± SEM, **p < 0.01. Lower panel, western blot showing the equal expression of CPT2 using COX IV as the mitochondrial protein marker.

(B) Interaction between SIRT3 and CPT2 (left) and reduced CPT2 acetylation (right) were detected in AML12 cells treated with LPA or control solution.

(C) Interaction between SIRT3 and CPT2 (left) and CPT2 acetylation (middle) were detected in primary mouse liver cells treated with LPA or control solution. CPT2 acetylation was quantified by ImageJ (right). n = 4, mean ± SEM, ***p < 0.001 versus Ctrl.

(D) Left, schematic illustration of site-specific mutations of SIRT3: Thr8 → Ala8, Ser17 → Ala17, or Thr8/ Ser17 → Ala8 and Ala17 using a site-directed mutagenesis kit (New England BioLabs Inc, Cat# E0554). Right, the expression level of acetylated CPT2 detected in AML12 cells expressing wild-type SIRT3, SIRT3-T8A or SIRT-S17A mutant, or SIRT3-T8A/S17A double mutants. In ImageJ quantitation, n = 4, mean ± SEM, **p < 0.01 versus Ctrl.

(E) Western blotting of SIRT3 in AML12 cells with two CRISPR/Cas9-mediated SIRT3 knockouts. CRISPR #1 (mSIRT3 #1 guide RNA) was used for subsequent experiments.

(F) Acetylated CPT2 proteins detected in SIRT3-KO AML12 cells rescued with wild-type SIRT3 (WT) or SIRT3-S17A mutant.

(G) CPT2 enzymatic activity measured by radiochemical assay in CRISPR/Cas9 SIRT3-KO AML12 cells re-expressing WT and mutant SIRT3 treated by LPA. The re-expressed proteins of wild-type SIRT3 (SIRT3 WT), SIRT3-T8A, SIRT-S17A, or SIRT3-T8A/S17A were verified by western blot of SIRT3 and β-actin as the loading control. n = 3, mean ± SEM, *p < 0.05, **p < 0.01 versus Ctrl.

See also Figure S6 and Table S4.

tested by rescuing CPT2-KO cells (Figure 6B; CRISPR-2; sgRNA-targeting sequences were shown in Table S4) with expression of WT CPT2 or mutants K453Q, K457Q, or K453Q and K457Q (Figures 6C and S6I). SIRT3-mediated CPT2 dimerization was indicted by a strong band of the v5-tag near 150 kDa detected in CRISPR-KO CPT2 cells reconstituted with v5-tag WT CPT2. However, such dimerization was greatly reduced in cells expressing CPT2-K453Q or CPT2-K457Q, where Q mimicked the constitutive acetylation that blocks deacetylation (Park et al., 2016), and absent in cells expressing the double CPT2-K453Q and K457Q mutant. In contrast, the dimerized CPT2 was enhanced in CPT2 cells with CPT2-K453R, K457R, or K453R and K457R with the Q-R mutation that enhances deacetylation (Figure 6D). CPT2 enzymatic activity measured by a ^{14}C-radiochemical assay further demonstrated that the 38% CPT2 activity remaining in the CPT2-KO cells was completely restored by expressing WT CPT2 and could be further enhanced by expression of deacetylation-mimic CPT2 mutants (K453R, K457R, or K453R/K457R). In consistence, WT CPT2 mediated restoration of CPT2 activity was absent in CPT2-KO cells reconstituted with acetylation mimics but restored in the deacetylation mimics (Figure 6E). Furthermore, FAO-driven oxygen consumption (Figure 6F) and mitochondrial ATP generation and OCR (Figure 6G) were completely enhanced by reconstitution of WT CPT2 but absent in the acetylation mimics. The CPT2 deacetylation mimics were also shown to be able to enhance mitochondrial metabolism (ATP generation, OCR, MnSOD activity, $\Delta\psi m$, and O_2^-) and cell viability in the absence of CDK1 and SIRT3 (Figures S6J–S6L). Collectively, these data provide the experimental evidence indicating that CPT2 K453/K457 are the sites of SIRT3-mediated CPT2 activation, which is required for CPT2 dimerization in LPA-induced mitochondrial metabolic enhancement.

DISCUSSION

In contrast to the popular conception of SFAs as deleterious to human health, this study reveals a beneficial effect induced by LPA on mitochondrial function and liver welfare. We report here that LPA promotes adaptive mitochondrial homeostasis that is able to ameliorate mitochondrial injuries induced by subsequent exposure to HPA or exposure to the hepatoxic agent CCl_4. In the CCl_4 mouse hepatotoxicity model, LPA-mediated adaptive mitochondrial activation lessens CCl_4-mediated liver injury with improved blood levels of ALT, AST, and m-AST.

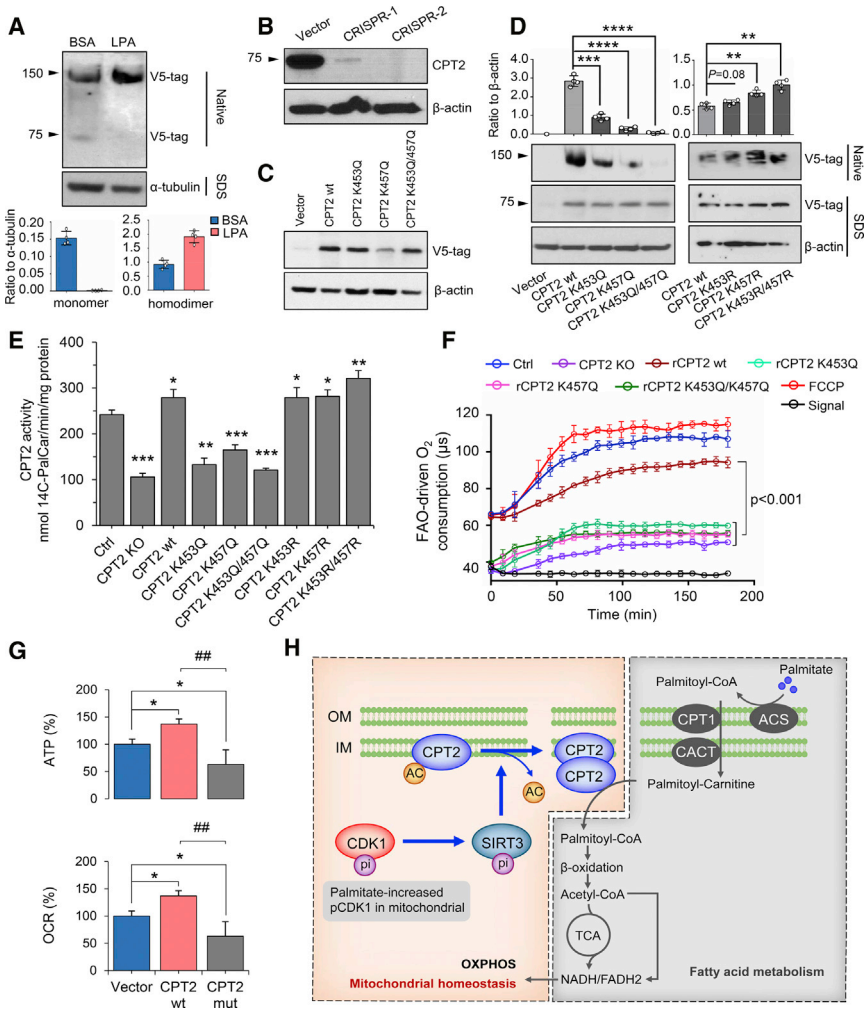

Figure 6. SIRT3-Mediated CPT2 Dimerization and Activation via Deacetylation at K453 and K457

(A) Enhanced CPT2 dimerization in AML12 cells transfected with v5-tag-labeled CPT2 and treated with LPA for 48 h. In ImageJ analysis, n = 4, mean ± SEM.

(B) Western blot of CPT2 in CRISPR/Cas9-edited CPT2 KO AML12 cells. CRISPR-2 with a complete CPT2 knockout was selected for subsequent experiments.

(C) Western blot of CPT2 in CPT2 KO cells reconstituted with v5-tag-labeled wild-type CPT2 (CPT2 WT), mutants K453Q or K457Q, or double mutant K453Q/K457Q.

(D) Formation of CPT2 homodimers in CRISPR-CPT2 knockout cells rescued with wild-type CPT2, mutants K453Q, K457Q, K453Q/K457Q or K453R, K457R, K453R/K457R that mutated back from K453Q, K457Q and K453Q/K457Q, respectively. Homodimers were quantified with ImageJ and normalized to α-tubulin, n = 4, mean ± SEM, $^{**}p < 0.01$, $^{***}p < 0.001$, $^{****}p < 0.0001$ versus CPT2 WT.

(E) CPT2 enzymatic activity as measured by ^{14}C radiochemical assay in LPA-treated cells compared with CPT2 knockout (KO) cells rescued with wild-type CPT2, mutants K453Q, K457Q, K453Q/K457Q or K453R, K457R, K453R/K457R that mutated back from K453Q, K457Q, and K453Q/K457Q, respectively. n = 3, mean ± SEM, $^{*}p < 0.05$, $^{**}p < 0.01$, $^{***}p < 0.001$ versus Ctrl.

(F) FAO-driven oxygen consumption was measured in LPA-treated CPT2 KO cells and the KO cells re-expressed WT or mutant (K453Q, K457Q, or K453Q/K457Q) CTP2. The uncoupler FCCP [Carbonyl cyanide-*4*-(trifluoromethoxy) phenylhydrazone] was used to induce maximal electron transport chain activity by dissipating $\Delta\psi m$. Signal and signal control (Ctrl) were used to show the probe signal in the absence of cellular respiration.

(G) ATP and OCR in LPA-treated CRISPR-CPT2 knockout AML12 cells rescued with wild-type (WT) CPT2 or K453Q/K457Q mutant. n = 3, mean ± SEM, $^{*}p < 0.05$ versus vector; $^{\#\#}p < 0.01$, $^{\#\#\#}p < 0.001$ versus CPT2 WT.

(H) CDK1-SIRT3-CPT2 cascade in LPA-promoted mitochondrial homeostasis. Findings from this study demonstrate a unique mechanism wherein mitochondrial homeostasis is maintained by a low concentration of PA (LPA). LPA enhances CDK1, which upregulates SIRT3 in mitochondria via Ser17 phosphorylation. CPT2 activity is then boosted by SIRT3-mediated deacetylation of CPT2 at K453/K457, causing CPT2 dimerization to accelerate CPT2 activity and FAO. OM, outer membrane; IM, inner membrane.

See also Figure S6 and Table S4.

The mechanistic insights of LPA-mediated mitochondrial homeostasis are revealed by uncovering two post-translational modifications in a unique CDK1-SIRT3-CPT2 cascade in which CDK1 activates SIRT3 via T8 and S17 phosphorylation that in turn leads to dimerization and activation of CPT2 via SIRT3-mediated CPT2 K453/K457 deacetylation (schematic presentation in Figure 6H).

Our present study sheds light on a long-held debate over the potential risk by consumption of SFAs (Nettleton et al., 2016). Reduction of dietary SFAs is recommended, although no evidence is indicated with SFA-mediated risk in cardiovascular disease. A possible reason for the overlooked pro-homeostatic benefit of SFAs is likely due to the comprehensive epidemiologic studies on SFA-related health risks and lipotoxic diseases associated with consumption of high-level SFAs (Kim et al., 2015; Kurahashi et al., 2008; Sellem et al., 2019). These studies were conducted with SFAs as a part of a fat-heavy diet with a prolonged period such as the population-based analysis on SFA-associated breast cancer risk (Sieri et al., 2014; Wakai et al., 2005). Another reason for the potentially advantageous function of SFAs being ignored may be the fact that ROS generated by SFAs cause widespread damage in cells (Yanagisawa et al., 2008). Therefore, it has been unclear whether an ideal physiological SFA consumption level required for maintaining normal mitochondrial and cellular function exists. Here, by lowering PA to a certain level, we reveal an obvious favorable function of PA for liver mitochondrial homeostasis. Compared to the enhanced ROS accumulation generated by HPA, mitochondrial superoxide is reduced with enhanced MnSOD, the major antioxidant enzyme in mitochondria, in LPA-mediated mitochondrial

protection. Broniarek et al. (2016) has found an enhanced MnSOD protein expression in endothelial cells induced by PA at 100 and 150 μM (Broniarek et al., 2016) that is consistent with our current finding that 100 μM PA increased MnSOD enzymatic activity by ~20% (Figure 1E). Importantly, 25 μM seems to be close to the physiological level, allowing AML12 cells to achieve the maximal mitochondrial and cellular protection. The doses near to 25 μM (12.5, 50, and 100 μM) also elevated MnSOD activity with related mitochondrial O_2^- alternations (Figure 1E). Such LPA-enhanced mitochondrial metabolism with boosted $\Delta\psi m$, OCR, and ATP generation are consistent with the findings that lowering the digestion of SFAs reduces health risk (Bueno et al., 2013). A small number of epidemiological studies of a low-fat diet (calories from fat <10%) show a benefit in weight loss and significant reduction of blood pressure as well as improving the ratio of total cholesterol to high-density lipoprotein (HDL) cholesterol (Shai et al., 2008). SFA-mediated cancer inhibition has also been demonstrated in human breast cancer cells (Evans et al., 2009; Levi et al., 2015). However, our current study revealed little improvement in mitochondrial function in cells treated with the PA in the dose range of 0–12.5 μM. These results seem to be consistent with the epidemical data showing that populations with less than 7% fat energy intake are no health benefit and, in most cases, an even worse disease burden (Figures 1A–1C and S1; Table S1). Although the exact definition of the physiology level of SFA consumption for humans will continue to debate and define, health benefits are evidenced by lowering fat intake (Tobias et al., 2015). Lieber and DeCarli (1970) demonstrated that 10% of total dietary calorie intake from FA, rather than either below or above such a level, generates the least hepatic triglyceride accumulation in rat liver (Lieber and DeCarli, 1970). A relative low-fat diet (<30% of energy) with 10% energy from SFAs is also recommended by WHO (https://www.who.int/en/news-room/fact-sheets/detail/healthy-diet), whereas dietary intake of <7% of energy from SFAs may be harmful (Dehghan et al., 2017).

Mitochondrial protein deacetylation plays a critical role in cell metabolism (De Marchi et al., 2019; Peek et al., 2013). SIRT3 is a NAD(+)-dependent deacetylase in the mitochondrial matrix to regulate the acetylation levels of metabolic enzymes. Hirschey et al. (2010) reported that LCAD is the metabolic substrate in SIRT3-regulated FAO metabolism during animal fasting (Hirschey et al., 2010). The current study further reveals that SIRT3-mediated dimerization is required for activation of another key FAO enzyme CPT2 via SIRT3-mediated deacetylation. The enhanced mitochondrial homeostasis was achieved at 48 h in cell culture and 12 days in animal tests, indicating that LPA exerts detectable cellular benefits in a time-dependent manner. Consistently, a similar lag time has been demonstrated in nutrition-derived cellular homeostasis (Morgan et al., 1998). In AMPK-mediated mitochondrial metabolism, non-glucose carbon sources limit mitochondrial biogenesis and OXPHOS capacity (Chaube et al., 2015), suggesting that a lag time is required for translating nutrition intake to detectable cellular benefits (Wang et al., 2011). In the present study, both phosphorylation and acetylation are involved in the LPA-mediated CDK1-SIRT3-CPT2 cascade, which may contribute to the lag time for orchestrating the mitochondrial homeostasis. CDK can regulate FA for cell cycle progression (Santos-Rosa et al., 2005), phosphorylate Drp1 to control mitochondrial dynamics (Tahbaz et al., 2011), and boost mitochondrial bioenergetics (Wang et al., 2014) and protein influx (Harbauer et al., 2014) for cell cycle progression. The mitochondrial CDK1, further defined in the current study, is enhanced by LPA to augment SIRT3 function via Thr8/Ser17 phosphorylation (Wang et al., 2014). Thus, CDK1-mediated SIRT3 phosphorylation may present the first rate-limiting step in LPA-promoted mitochondrial homeostasis. SIRT3-mediated deacetylation and activation of CPT2 may also contribute to the lag time for LPA-mediated mitochondrial activation. In addition, the cluster of mitochondrial proteins including factors for redox balance and FA metabolism detected from our proteomics analysis suggests multiple metabolic mechanisms involved in LPA-mediated mitochondrial function. Further elucidation of such pro-homeostatic factors related to CDK1-SIRT3-CPT2 cascade will be necessary to reveal more mechanistic insights in LPA-mediated mitochondrial homeostasis.

The LPA-mediated protective function against the injuries induced by HPA or CCl_4 may have a critical clinical impact. SIRT3 is the central regulator of mitochondrial homeostasis (Newman et al., 2012) that can regulate FAO metabolism (Hallows et al., 2011) and MnSOD activation (Tao et al., 2010) as well as LCAD (Bharathi et al., 2013). Increased risk of developing metabolic syndrome is observed in humans with a deficiency of SIRT3 (Hirschey et al., 2011). The reported SIRT3-mediated MnSOD activation (Tao et al., 2010) is also involved in the LPA-mediated mitochondrial homeostasis probably due to the requirement of detoxifying the enhanced O_2^- level of FAO and mitochondrial respiration. Thus, SIRT3-mediated MnSOD activation may play a key role in the LPA-mediated mitochondrial protective function against lipotoxicity induced by HPA or the hepatotoxic effect induced by CCL_4.

SIRT3 is reported to be involved in FAO metabolism (Hirschey et al., 2010). Additionally, two recent works are supportive to our current findings, indicating the importance of fatty acid turnover rate in the maintenance of human weight and health (Arner et al., 2019) and the critical role of SIRT3 in controlling mitochondrial metabolism via protein deacetylation (Wang et al., 2019). Our results further demonstrate that CPT2 is directly controlled by SIRT3 in LPA-mediated mitochondrial homeostasis via deacetylation-controlled dimerization enzyme activity. CPT2 located in the inner mitochondrial membrane functions in lipid mitochondrial transportation and oxidization, which is connected to the TCA cycle and mitochondrial bioenergetics. CPT2-mediated FA metabolism is demonstrated in an array of cellular functions (Gonzalez-Hurtado et al., 2018; Xiong et al., 2018). Defects in the CPT2 gene are associated with deficiency in mitochondrial FAO and impair the functions of complexes I and V (Haorah et al., 2013). SIRT3-mediated deacetylation is found to be necessary for CPT2 dimerization and enzymatic activation. Such post-translational modification of CPT2 in mitochondria does not require gene transcription, and thus CPT2 protein levels are not necessarily enhanced in LPA-treated cells. Thus, the SIRT3-mediated deacetylation and dimerization of CPT2 indicates a quick regulatory mechanism on FAO enhancement. In addition, SIRT3-mediated CPT2 deacetylation and activation is nonetheless related to the CPT1 activity that regulates the rate of FA import into the mitochondria from the cytoplasm. The

mechanistic insights regulating the coupling between CPT1 and CPT2 in LPA-mediated mitochondrial FAO is to be further elucidated.

In conclusion, this study uncovered an overlooked beneficial effect of SFAs on mitochondrial homeostasis that alleviates HPA-induced lipotoxic effect and CCL_4-induced hepatotoxicity. A unique pathway CDK1-SIRT3-CPT2 is identified in LPA-mediated mitochondrial metabolic enhancement.

SUPPORTING CITATIONS

Akazawa et al., 2010; Barreyro et al., 2007; Borradaile et al., 2006a, 2006b; Brookheart et al., 2009; Bunn et al., 2010; Cacicedo et al., 2005; Egnatchik et al., 2014; El-Assaad et al., 2003; Esposito et al., 2009; Gao et al., 2010; Igoillo-Esteve et al., 2010; Inoguchi et al., 2000; Inoue et al., 2005; Listenberger et al., 2001; Malhi et al., 2006; Mantena et al., 2009; Marwarha et al., 2016; Park et al., 2010; Pfaffenbach et al., 2010; Pfluger et al., 2008; Wang et al., 2006, 2008; Wei et al., 2009; Weigert et al., 2004; Wen et al., 2011; Xu et al., 2010

STAR★METHODS

Detailed methods are provided in the online version of this paper and include the following:

- KEY RESOURCES TABLE
- LEAD CONTACT AND MATERIALS AVAILABILITY
- EXPERIMENTAL MODEL AND SUBJECT DETAILS
  - Cells
  - Animals
  - Preparation and Administration of Palmitate
  - CCl_4-Induced Cytotoxicity and Hepatotoxicity
- METHOD DETAILS
  - Mitochondrial Protein Preparation
  - LPA-Mediated Mitochondrial Proteomics
  - Data Analysis on Mitochondrial Proteomics
  - ATP Generation
  - OCR
  - MnSOD Enzyme Activity
  - Mitochondrial Membrane Potential, $\Delta\psi m$
  - Mitochondrial O_2^- Production
  - MTT Assay
  - Oil red O Staining and Quantitation
  - Detection of PA in Mouse Liver Tissue by UPLC-TQMS
  - Coimmunoprecipitation and Western Blotting
  - Mitochondrial–GFP Confocal Microscopy
  - Transmission Electron Microscopy
  - Measurements of ALT, AST, and m-AST
  - Hematoxylin and Eosin (H&E) Staining
  - CPT2 Activity
  - CRISPR/Cas9-Mediated Gene Editing
  - Native PAGE and Western Blotting
  - FAO-Driven Oxygen Consumption
  - Plasmid Construction
- QUANTIFICATION AND STATISTICAL ANALYSIS
- DATA AND CODE AVAILABILITY

SUPPLEMENTAL INFORMATION

Supplemental Information can be found online at https://doi.org/10.1016/j.devcel.2019.11.012.

ACKNOWLEDGMENTS

This work was supported in part by National Cancer Institute grant R01 CA213830 (to J.J.L.), Natural Science Foundation of China grant NSFC 81673765 (to Y.H.), and the UC Davis Comprehensive Cancer Center Support Grant (CCCSG) awarded by the National Cancer Institute (NCI P30CA093373) for sharing facilities. The authors thank Dr. Andrew Vaughan, Dr. John Rutledge, Mr. Jie Hunter Huang, and Dr. Aris Alexandrou for their critical review of the manuscript and technical assistance.

AUTHOR CONTRIBUTIONS

J.J.L. contributed to the conception of the project and guided the experiments. L.L., B.X., and M.F. performed most of the experiments with assistance from D.C.-G. Y.H., J.J.L., L.L., and B.X. designed and performed the *in vivo* mouse tests. J.X.J. contributed to the preparation and characterization of hepatocytes isolated from mouse livers. Y.W. and R.W. did the mitochondrial proteomics assay and data analysis. H.-W.C. guided the designing of CRISPR/Cas9 knockout experiments and provided the CRISPR constructs. L.L., B.X., and M.F. generated the SIRT3 and CPT2 CRISPR/Cas9 knockout AML12 cells as well as the mutant SIRT3 and CPT2 cells. L.L., B.X., and J.J.L. interpreted the data and wrote the manuscript. All authors reviewed the manuscript.

DECLARATION OF INTERESTS

The authors declare no competing interests.

Received: September 3, 2018
Revised: October 10, 2019
Accepted: November 18, 2019
Published: December 19, 2019

REFERENCES

Akazawa, Y., Cazanave, S., Mott, J.L., Elmi, N., Bronk, S.F., Kohno, S., Charlton, M.R., and Gores, G.J. (2010). Palmitoleate attenuates palmitate-induced Bim and PUMA up-regulation and hepatocyte lipoapoptosis. J. Hepatol. *52*, 586–593.

Arner, P., Bernard, S., Appelsved, L., Fu, K.Y., Andersson, D.P., Salehpour, M., Thorell, A., Rydén, M., and Spalding, K.L. (2019). Adipose lipid turnover and long-term changes in body weight. Nat. Med. *25*, 1385–1389.

Bao, J., Scott, I., Lu, Z., Pang, L., Dimond, C.C., Gius, D., and Sack, M.N. (2010). SIRT3 is regulated by nutrient excess and modulates hepatic susceptibility to lipotoxicity. Free Radic. Biol. Med. *49*, 1230–1237.

Barreyro, F.J., Kobayashi, S., Bronk, S.F., Werneburg, N.W., Malhi, H., and Gores, G.J. (2007). Transcriptional regulation of Bim by FoxO3A mediates hepatocyte lipoapoptosis. J. Biol. Chem. *282*, 27141–27154.

Berardi, M.J., and Chou, J.J. (2014). Fatty acid flippase activity of UCP2 is essential for its proton transport in mitochondria. Cell Metab. *20*, 541–552.

Bharathi, S.S., Zhang, Y., Mohsen, A.W., Uppala, R., Balasubramani, M., Schreiber, E., Uechi, G., Beck, M.E., Rardin, M.J., Vockley, J., et al. (2013). Sirtuin 3 (SIRT3) protein regulates long-chain acyl-CoA dehydrogenase by deacetylating conserved lysines near the active site. J. Biol. Chem. *288*, 33837–33847.

Borradaile, N.M., Buhman, K.K., Listenberger, L.L., Magee, C.J., Morimoto, E.T., Ory, D.S., and Schaffer, J.E. (2006a). A critical role for eukaryotic elongation factor 1A-1 in lipotoxic cell death. Mol. Biol. Cell *17*, 770–778.

Borradaile, N.M., Han, X., Harp, J.D., Gale, S.E., Ory, D.S., and Schaffer, J.E. (2006b). Disruption of endoplasmic reticulum structure and integrity in lipotoxic cell death. J. Lipid Res. *47*, 2726–2737.

Brenmoehl, J., and Hoeflich, A. (2013). Dual control of mitochondrial biogenesis by sirtuin 1 and sirtuin 3. Mitochondrion *13*, 755–761.

Broniarek, I., Koziel, A., and Jarmuszkiewicz, W. (2016). The effect of chronic exposure to high palmitic acid concentrations on the aerobic metabolism of human endothelial EA.hy926 cells. Pflugers Arch. *468*, 1541–1554.

Brookheart, R.T., Michel, C.I., Listenberger, L.L., Ory, D.S., and Schaffer, J.E. (2009). The non-coding RNA gadd7 is a regulator of lipid-induced oxidative and endoplasmic reticulum stress. J. Biol. Chem. *284*, 7446–7454.

Bueno, N.B., de Melo, I.S., de Oliveira, S.L., and da Rocha Ataide, T. (2013). Very-low-carbohydrate ketogenic diet v. low-fat diet for long-term weight loss: a meta-analysis of randomised controlled trials. Br. J. Nutr. *110*, 1178–1187.

Bunn, R.C., Cockrell, G.E., Ou, Y., Thrailkill, K.M., Lumpkin, C.K., Jr., and Fowlkes, J.L. (2010). Palmitate and insulin synergistically induce IL-6 expression in human monocytes. Cardiovasc. Diabetol. *9*, 73.

Cacicedo, J.M., Benjachareowong, S., Chou, E., Ruderman, N.B., and Ido, Y. (2005). Palmitate-induced apoptosis in cultured bovine retinal pericytes: roles of NAD(P)H oxidase, oxidant stress, and ceramide. Diabetes *54*, 1838–1845.

Chaube, B., Malvi, P., Singh, S.V., Mohammad, N., Viollet, B., and Bhat, M.K. (2015). AMPK maintains energy homeostasis and survival in cancer cells via regulating p38/PGC-1alpha-mediated mitochondrial biogenesis. Cell Death Discov. *1*, 15063.

Corbet, C., Pinto, A., Martherus, R., Santiago de Jesus, J.P., Polet, F., and Feron, O. (2016). Acidosis drives the reprogramming of fatty acid metabolism in cancer cells through changes in mitochondrial and histone acetylation. Cell Metab. *24*, 311–323.

Cox, J., and Mann, M. (2008). MaxQuant enables high peptide identification rates, individualized p.p.b.-range mass accuracies and proteome-wide protein quantification. Nat. Biotechnol. *26*, 1367–1372.

De Marchi, U., Galindo, A.N., Thevenet, J., Hermant, A., Bermont, F., Lassueur, S., Domingo, J.S., Kussmann, M., Dayon, L., and Wiederkehr, A. (2019). Mitochondrial lysine deacetylation promotes energy metabolism and calcium signaling in insulin-secreting cells. FASEB J. *33*, 4660–4674.

de Souza, R.J., Mente, A., Maroleanu, A., Cozma, A.I., Ha, V., Kishibe, T., Uleryk, E., Budylowski, P., Schünemann, H., Beyene, J., et al. (2015). Intake of saturated and trans unsaturated fatty acids and risk of all cause mortality, cardiovascular disease, and type 2 diabetes: systematic review and meta-analysis of observational studies. BMJ *351*, h3978.

Dehghan, M., Mente, A., Zhang, X., Swaminathan, S., Li, W., Mohan, V., Iqbal, R., Kumar, R., Wentzel-Viljoen, E., Rosengren, A., et al. (2017). Associations of fats and carbohydrate intake with cardiovascular disease and mortality in 18 countries from five continents (PURE): a prospective cohort study. Lancet *390*, 2050–2062.

Domenicali, M., Caraceni, P., Giannone, F., Baldassarre, M., Lucchetti, G., Quarta, C., Patti, C., Catani, L., Nanni, C., Lemoli, R.M., et al. (2009). A novel model of CCl4-induced cirrhosis with ascites in the mouse. J. Hepatol. *51*, 991–999.

Egnatchik, R.A., Leamy, A.K., Jacobson, D.A., Shiota, M., and Young, J.D. (2014). ER calcium release promotes mitochondrial dysfunction and hepatic cell lipotoxicity in response to palmitate overload. Mol. Metab. *3*, 544–553.

El-Assaad, W., Buteau, J., Peyot, M.L., Nolan, C., Roduit, R., Hardy, S., Joly, E., Dbaibo, G., Rosenberg, L., and Prentki, M. (2003). Saturated fatty acids synergize with elevated glucose to cause pancreatic beta-cell death. Endocrinology *144*, 4154–4163.

Esposito, E., Iacono, A., Bianco, G., Autore, G., Cuzzocrea, S., Vajro, P., Canani, R.B., Calignano, A., Raso, G.M., and Meli, R. (2009). Probiotics reduce the inflammatory response induced by a high-fat diet in the liver of young rats. J. Nutr. *139*, 905–911.

Evans, L.M., Toline, E.C., Desmond, R., Siegal, G.P., Hashim, A.I., and Hardy, R.W. (2009). Dietary stearate reduces human breast cancer metastasis burden in athymic nude mice. Clin. Exp. Metastasis *26*, 415–424.

Forouhi, N.G., Koulman, A., Sharp, S.J., Imamura, F., Kröger, J., Schulze, M.B., Crowe, F.L., Huerta, J.M., Guevara, M., Beulens, J.W., et al. (2014). Differences in the prospective association between individual plasma phospholipid saturated fatty acids and incident type 2 diabetes: the EPIC-InterAct case-cohort study. Lancet Diabetes Endocrinol. *2*, 810–818.

Gao, D., Nong, S., Huang, X., Lu, Y., Zhao, H., Lin, Y., Man, Y., Wang, S., Yang, J., and Li, J. (2010). The effects of palmitate on hepatic insulin resistance are mediated by NADPH oxidase 3-derived reactive oxygen species through JNK and p38MAPK pathways. J. Biol. Chem. *285*, 29965–29973.

Geng, T., Sutter, A., Harland, M.D., Law, B.A., Ross, J.S., Lewin, D., Palanisamy, A., Russo, S.B., Chavin, K.D., and Cowart, L.A. (2015). Sphingosine kinase 1 mediates hepatic inflammation in a mouse model of nonalcoholic steatohepatitis induced by high saturated fat feeding and initiates proinflammatory signaling in hepatocytes. J. Lipid Res. *56*, 2359–2371.

Gonzalez-Hurtado, E., Lee, J., Choi, J., and Wolfgang, M.J. (2018). Fatty acid oxidation is required for active and quiescent brown adipose tissue maintenance and thermogenic programing. Mol. Metab. *7*, 45–56.

Graier, W.F., Malli, R., and Kostner, G.M. (2009). Mitochondrial protein phosphorylation: instigator or target of lipotoxicity? Trends Endocrinol. Metab. *20*, 186–193.

Hallows, W.C., Yu, W., Smith, B.C., Devries, M.K., Ellinger, J.J., Someya, S., Shortreed, M.R., Prolla, T., Markley, J.L., Smith, L.M., et al. (2011). Sirt3 promotes the urea cycle and fatty acid oxidation during dietary restriction. Mol. Cell *41*, 139–149.

Haorah, J., Rump, T.J., and Xiong, H. (2013). Reduction of brain mitochondrial beta-oxidation impairs complex I and V in chronic alcohol intake: the underlying mechanism for neurodegeneration. PLoS One *8*, e70833.

Harbauer, A.B., Opalińska, M., Gerbeth, C., Herman, J.S., Rao, S., Schönfisch, B., Guiard, B., Schmidt, O., Pfanner, N., and Meisinger, C. (2014). Mitochondria. Cell cycle-dependent regulation of mitochondrial preprotein translocase. Science *346*, 1109–1113.

Hirschey, M.D., Shimazu, T., Goetzman, E., Jing, E., Schwer, B., Lombard, D.B., Grueter, C.A., Harris, C., Biddinger, S., Ilkayeva, O.R., et al. (2010). SIRT3 regulates mitochondrial fatty-acid oxidation by reversible enzyme deacetylation. Nature *464*, 121–125.

Hirschey, M.D., Shimazu, T., Jing, E., Grueter, C.A., Collins, A.M., Aouizerat, B., Stančáková, A., Goetzman, E., Lam, M.M., Schwer, B., et al. (2011). SIRT3 deficiency and mitochondrial protein hyperacetylation accelerate the development of the metabolic syndrome. Mol. Cell *44*, 177–190.

Hsiao, Y.S., Jogl, G., Esser, V., and Tong, L. (2006). Crystal structure of rat carnitine palmitoyltransferase II (CPT-II). Biochem. Biophys. Res. Commun. *346*, 974–980.

Igoillo-Esteve, M., Marselli, L., Cunha, D.A., Ladrière, L., Ortis, F., Grieco, F.A., Dotta, F., Weir, G.C., Marchetti, P., Eizirik, D.L., et al. (2010). Palmitate induces a pro-inflammatory response in human pancreatic islets that mimics CCL2 expression by beta cells in type 2 diabetes. Diabetologia *53*, 1395–1405.

Imamura, F., Sharp, S.J., Koulman, A., Schulze, M.B., Kröger, J., Griffin, J.L., Huerta, J.M., Guevara, M., Sluijs, I., Agudo, A., et al. (2017). A combination of plasma phospholipid fatty acids and its association with incidence of type 2 diabetes: the EPIC-InterAct case-cohort study. PLoS Med. *14*, e1002409.

Inoguchi, T., Li, P., Umeda, F., Yu, H.Y., Kakimoto, M., Imamura, M., Aoki, T., Etoh, T., Hashimoto, T., Naruse, M., et al. (2000). High glucose level and free fatty acid stimulate reactive oxygen species production through protein kinase C–dependent activation of NAD(P)H oxidase in cultured vascular cells. Diabetes *49*, 1939–1945.

Inoue, M., Ohtake, T., Motomura, W., Takahashi, N., Hosoki, Y., Miyoshi, S., Suzuki, Y., Saito, H., Kohgo, Y., and Okumura, T. (2005). Increased expression of PPARgamma in high fat diet-induced liver steatosis in mice. Biochem. Biophys. Res. Commun. *336*, 215–222.

Kim, F., Pham, M., Luttrell, I., Bannerman, D.D., Tupper, J., Thaler, J., Hawn, T.R., Raines, E.W., and Schwartz, M.W. (2007). Toll-like receptor-4 mediates vascular inflammation and insulin resistance in diet-induced obesity. Circ. Res. *100*, 1589–1596.

Kim, H.S., Patel, K., Muldoon-Jacobs, K., Bisht, K.S., Aykin-Burns, N., Pennington, J.D., van der Meer, R., Nguyen, P., Savage, J., Owens, K.M., et al. (2010). SIRT3 is a mitochondria-localized tumor suppressor required for maintenance of mitochondrial integrity and metabolism during stress. Cancer Cell *17*, 41–52.

Kim, S.R., Jeon, S.Y., and Lee, S.M. (2015). The association of cardiovascular risk factors with saturated fatty acids and fatty acid desaturase indices in erythrocyte in middle-aged Korean adults. Lipids Health Dis. *14*, 133.

Knockaert, L., Berson, A., Ribault, C., Prost, P.E., Fautrel, A., Pajaud, J., Lepage, S., Lucas-Clerc, C., Bégué, J.M., Fromenty, B., et al. (2012). Carbon tetrachloride-mediated lipid peroxidation induces early mitochondrial alterations in mouse liver. Lab. Invest. *92*, 396–410.

Koyama, T., Kume, S., Koya, D., Araki, S., Isshiki, K., Chin-Kanasaki, M., Sugimoto, T., Haneda, M., Sugaya, T., Kashiwagi, A., et al. (2011). SIRT3 attenuates palmitate-induced ROS production and inflammation in proximal tubular cells. Free Radic. Biol. Med. *51*, 1258–1267.

Kurahashi, N., Inoue, M., Iwasaki, M., Sasazuki, S., and Tsugane, A.S.; Japan Public Health Center-Based Prospective Study Group (2008). Dairy product, saturated fatty acid, and calcium intake and prostate cancer in a prospective cohort of Japanese men. Cancer Epidemiol. Biomarkers Prev *17*, 930–937.

Kwan, H.Y., Hu, Y.M., Chan, C.L., Cao, H.H., Cheng, C.Y., Pan, S.Y., Tse, K.W., Wu, Y.C., Yu, Z.L., and Fong, W.F. (2013). Lipidomics identification of metabolic biomarkers in chemically induced hypertriglyceridemic mice. J. Proteome Res. *12*, 1387–1398.

Leamy, A.K., Egnatchik, R.A., Shiota, M., Ivanova, P.T., Myers, D.S., Brown, H.A., and Young, J.D. (2014). Enhanced synthesis of saturated phospholipids is associated with ER stress and lipotoxicity in palmitate treated hepatic cells. J. Lipid Res. *55*, 1478–1488.

Lee, J.E., Spiegelman, D., Hunter, D.J., Albanes, D., Bernstein, L., van den Brandt, P.A., Buring, J.E., Cho, E., English, D.R., Freudenheim, J.L., et al. (2008). Fat, protein, and meat consumption and renal cell cancer risk: a pooled analysis of 13 prospective studies. J. Natl. Cancer Inst. *100*, 1695–1706.

Levi, L., Wang, Z., Doud, M.K., Hazen, S.L., and Noy, N. (2015). Saturated fatty acids regulate retinoic acid signalling and suppress tumorigenesis by targeting fatty acid-binding protein 5. Nat. Commun. *6*, 8794.

Lieber, C.S., and DeCarli, L.M. (1970). Quantitative relationship between amount of dietary fat and severity of alcoholic fatty liver. Am. J. Clin. Nutr. *23*, 474–478.

Lin, L., Ding, Y., Wang, Y., Wang, Z., Yin, X., Yan, G., Zhang, L., Yang, P., and Shen, H. (2017). Functional lipidomics: palmitic acid impairs hepatocellular carcinoma development by modulating membrane fluidity and glucose metabolism. Hepatology *66*, 432–448.

Linder, M.E., and Deschenes, R.J. (2007). Palmitoylation: policing protein stability and traffic. Nat. Rev. Mol. Cell Biol. *8*, 74–84.

Listenberger, L.L., Ory, D.S., and Schaffer, J.E. (2001). Palmitate-induced apoptosis can occur through a ceramide-independent pathway. J. Biol. Chem. *276*, 14890–14895.

Liu, R., Fan, M., Candas, D., Qin, L., Zhang, X., Eldridge, A., Zou, J.X., Zhang, T., Juma, S., Jin, C., et al. (2015). CDK1-mediated SIRT3 activation enhances mitochondrial function and tumor radioresistance. Mol. Cancer Ther. *14*, 2090–2102.

Malhi, H., Bronk, S.F., Werneburg, N.W., and Gores, G.J. (2006). Free fatty acids induce JNK-dependent hepatocyte lipoapoptosis. J. Biol. Chem. *281*, 12093–12101.

Mancini, A., Imperlini, E., Nigro, E., Montagnese, C., Daniele, A., Orrù, S., and Buono, P. (2015). Biological and nutritional properties of palm oil and palmitic acid: effects on health. Molecules *20*, 17339–17361.

Mantena, S.K., Vaughn, D.P., Andringa, K.K., Eccleston, H.B., King, A.L., Abrams, G.A., Doeller, J.E., Kraus, D.W., Darley-Usmar, V.M., and Bailey, S.M. (2009). High fat diet induces dysregulation of hepatic oxygen gradients and mitochondrial function in vivo. Biochem. J. *417*, 183–193.

Marwarha, G., Claycombe, K., Schommer, J., Collins, D., and Ghribi, O. (2016). Palmitate-induced endoplasmic reticulum stress and subsequent C/EBPalpha homologous protein activation attenuates leptin and insulin-like growth factor 1 expression in the brain. Cell. Signal. *28*, 1789–1805.

Morales-Garza, L.A., Puche, J.E., Aguirre, G.A., Muñoz, Ú., García-Magariño, M., De la Garza, R.G., and Castilla-Cortazar, I. (2017). Experimental approach to IGF-1 therapy in CCl4-induced acute liver damage in healthy controls and mice with partial IGF-1 deficiency. J. Transl. Med. *15*, 96.

Morgan, L., Arendt, J., Owens, D., Folkard, S., Hampton, S., Deacon, S., English, J., Ribeiro, D., and Taylor, K. (1998). Effects of the endogenous clock and sleep time on melatonin, insulin, glucose and lipid metabolism. J. Endocrinol. *157*, 443–451.

Mota, M., Banini, B.A., Cazanave, S.C., and Sanyal, A.J. (2016). Molecular mechanisms of lipotoxicity and glucotoxicity in nonalcoholic fatty liver disease. Metabolism *65*, 1049–1061.

Nettleton, J.A., Lovegrove, J.A., Mensink, R.P., and Schwab, U. (2016). Dietary fatty acids: is it time to change the recommendations? Ann. Nutr. Metab. *68*, 249–257.

Newman, J.C., He, W., and Verdin, E. (2012). Mitochondrial protein acylation and intermediary metabolism: regulation by sirtuins and implications for metabolic disease. J. Biol. Chem. *287*, 42436–42443.

Noakes, T.D., and Windt, J. (2017). Evidence that supports the prescription of low-carbohydrate high-fat diets: a narrative review. Br. J. Sports Med. *51*, 133–139.

O'Shea, R.S., Dasarathy, S., and McCullough, A.J.; Practice Guideline Committee of the American Association for the Study of Liver Diseases; Practice Parameters Committee of the American College of Gastroenterology (2010). Alcoholic liver disease. Hepatology *51*, 307–328.

Ozden, O., Park, S.H., Kim, H.S., Jiang, H., Coleman, M.C., Spitz, D.R., and Gius, D. (2011). Acetylation of MnSOD directs enzymatic activity responding to cellular nutrient status or oxidative stress. Aging (Albany, NY) *3*, 102–107.

Park, E.J., Lee, J.H., Yu, G.Y., He, G., Ali, S.R., Holzer, R.G., Osterreicher, C.H., Takahashi, H., and Karin, M. (2010). Dietary and genetic obesity promote liver inflammation and tumorigenesis by enhancing IL-6 and TNF expression. Cell *140*, 197–208.

Park, S.H., Ozden, O., Liu, G., Song, H.Y., Zhu, Y., Yan, Y., Zou, X., Kang, H.J., Jiang, H., Principe, D.R., et al. (2016). SIRT2-mediated deacetylation and tetramerization of pyruvate kinase directs glycolysis and tumor growth. Cancer Res. *76*, 3802–3812.

Peek, C.B., Affinati, A.H., Ramsey, K.M., Kuo, H.Y., Yu, W., Sena, L.A., Ilkayeva, O., Marcheva, B., Kobayashi, Y., Omura, C., et al. (2013). Circadian clock NAD^+ cycle drives mitochondrial oxidative metabolism in mice. Science *342*, 1243417.

Pfaffenbach, K.T., Gentile, C.L., Nivala, A.M., Wang, D., Wei, Y., and Pagliassotti, M.J. (2010). Linking endoplasmic reticulum stress to cell death in hepatocytes: roles of C/EBP homologous protein and chemical chaperones in palmitate-mediated cell death. Am. J. Physiol. Endocrinol. Metab. *298*, E1027–E1035.

Pfluger, P.T., Herranz, D., Velasco-Miguel, S., Serrano, M., and Tschöp, M.H. (2008). Sirt1 protects against high-fat diet-induced metabolic damage. Proc. Natl. Acad. Sci. USA *105*, 9793–9798.

Qin, L., Fan, M., Candas, D., Jiang, G., Papadopoulos, S., Tian, L., Woloschak, G., Grdina, D.J., and Li, J.J. (2015). CDK1 enhances mitochondrial bioenergetics for radiation-induced DNA repair. Cell Rep. *13*, 2056–2063.

Qiu, X., Brown, K., Hirschey, M.D., Verdin, E., and Chen, D. (2010). Calorie restriction reduces oxidative stress by SIRT3-mediated SOD2 activation. Cell Metab. *12*, 662–667.

Santos-Rosa, H., Leung, J., Grimsey, N., Peak-Chew, S., and Siniossoglou, S. (2005). The yeast lipin Smp2 couples phospholipid biosynthesis to nuclear membrane growth. EMBO J. *24*, 1931–1941.

Sellem, L., Srour, B., Guéraud, F., Pierre, F., Kesse-Guyot, E., Fiolet, T., Lavalette, C., Egnell, M., Latino-Martel, P., Fassier, P., et al. (2019). Saturated, mono- and polyunsaturated fatty acid intake and cancer risk: results from the French prospective cohort NutriNet-Sante. Eur. J. Nutr. *58*, 1515–1527.

Senyilmaz, D., Virtue, S., Xu, X., Tan, C.Y., Griffin, J.L., Miller, A.K., Vidal-Puig, A., and Teleman, A.A. (2015). Regulation of mitochondrial morphology and function by stearoylation of TFR1. Nature *525*, 124–128.

Shai, I., Schwarzfuchs, D., Henkin, Y., Shahar, D.R., Witkow, S., Greenberg, I., Golan, R., Fraser, D., Bolotin, A., Vardi, H., et al. (2008). Weight loss with a low-carbohydrate, Mediterranean, or low-fat diet. N. Engl. J. Med. *359*, 229–241.

Sieri, S., Chiodini, P., Agnoli, C., Pala, V., Berrino, F., Trichopoulou, A., Benetou, V., Vasilopoulou, E., Sánchez, M.J., Chirlaque, M.D., et al. (2014). Dietary fat intake and development of specific breast cancer subtypes. J. Natl. Cancer Inst. *106*, dju068.

Siri-Tarino, P.W., Sun, Q., Hu, F.B., and Krauss, R.M. (2010). Meta-analysis of prospective cohort studies evaluating the association of saturated fat with cardiovascular disease. Am. J. Clin. Nutr. *91*, 535–546.

Spitz, D.R., and Oberley, L.W. (2001). Measurement of MnSOD and CuZnSOD activity in mammalian tissue homogenates. Curr. Protoc. Toxicol. 7.5.1–7.5.11.

Tahbaz, N., Subedi, S., and Weinfeld, M. (2011). Role of polynucleotide kinase/phosphatase in mitochondrial DNA repair. Nucleic Acids Res. *8*, 3484–3495.

Tao, R., Coleman, M.C., Pennington, J.D., Ozden, O., Park, S.H., Jiang, H., Kim, H.S., Flynn, C.R., Hill, S., Hayes McDonald, W., et al. (2010). Sirt3-mediated deacetylation of evolutionarily conserved lysine 122 regulates MnSOD activity in response to stress. Mol. Cell *40*, 893–904.

Tobias, D.K., Chen, M., Manson, J.E., Ludwig, D.S., Willett, W., and Hu, F.B. (2015). Effect of low-fat diet interventions versus other diet interventions on long-term weight change in adults: a systematic review and meta-analysis. Lancet Diabetes Endocrinol. *3*, 968–979.

Wakai, K., Tamakoshi, K., Date, C., Fukui, M., Suzuki, S., Lin, Y., Niwa, Y., Nishio, K., Yatsuya, H., Kondo, T., et al. (2005). Dietary intakes of fat and fatty acids and risk of breast cancer: a prospective study in Japan. Cancer Sci. *96*, 590–599.

Wang, D., Wei, Y., and Pagliassotti, M.J. (2006). Saturated fatty acids promote endoplasmic reticulum stress and liver injury in rats with hepatic steatosis. Endocrinology *147*, 943–951.

Wang, Y., Ausman, L.M., Russell, R.M., Greenberg, A.S., and Wang, X.D. (2008). Increased apoptosis in high-fat diet-induced nonalcoholic steatohepatitis in rats is associated with c-Jun NH2-terminal kinase activation and elevated proapoptotic Bax. J. Nutr. *138*, 1866–1871.

Wang, R., Dillon, C.P., Shi, L.Z., Milasta, S., Carter, R., Finkelstein, D., McCormick, L.L., Fitzgerald, P., Chi, H., Munger, J., et al. (2011). The transcription factor Myc controls metabolic reprogramming upon T lymphocyte activation. Immunity *35*, 871–882.

Wang, J., Zou, J.X., Xue, X., Cai, D., Zhang, Y., Duan, Z., Xiang, Q., Yang, J.C., Louie, M.C., Borowsky, A.D., et al. (2016). ROR-gamma drives androgen receptor expression and represents a therapeutic target in castration-resistant prostate cancer. Nat. Med. *22*, 488–496.

Wang, T., Cao, Y., Zheng, Q., Tu, J., Zhou, W., He, J., Zhong, J., Chen, Y., Wang, J., Cai, R., et al. (2019). SENP1-Sirt3 signaling controls mitochondrial protein acetylation and metabolism. Mol. Cell *75*, 823–834.e5.

Wang, Z., Fan, M., Candas, D., Zhang, T.Q., Qin, L., Eldridge, A., Wachsmann-Hogiu, S., Ahmed, K.M., Chromy, B.A., Nantajit, D., et al. (2014). Cyclin B1/Cdk1 coordinates mitochondrial respiration for cell-cycle G2/M progression. Dev. Cell *29*, 217–232.

Wei, Y., Wang, D., Gentile, C.L., and Pagliassotti, M.J. (2009). Reduced endoplasmic reticulum luminal calcium links saturated fatty acid-mediated endoplasmic reticulum stress and cell death in liver cells. Mol. Cell. Biochem. *331*, 31–40.

Weigert, C., Brodbeck, K., Staiger, H., Kausch, C., Machicao, F., Häring, H.U., and Schleicher, E.D. (2004). Palmitate, but not unsaturated fatty acids, induces the expression of interleukin-6 in human myotubes through proteasome-dependent activation of nuclear factor-kappaB. J. Biol. Chem. *279*, 23942–23952.

Wen, H., Gris, D., Lei, Y., Jha, S., Zhang, L., Huang, M.T., Brickey, W.J., and Ting, J.P. (2011). Fatty acid-induced NLRP3-ASC inflammasome activation interferes with insulin signaling. Nat. Immunol. *12*, 408–415.

Willett, W.C., Stampfer, M.J., and Sacks, F.M. (2014). Association of dietary, circulating, and supplement fatty acids with coronary risk. Ann. Intern. Med. *161*, 453.

Winnik, S., Auwerx, J., Sinclair, D.A., and Matter, C.M. (2015). Protective effects of sirtuins in cardiovascular diseases: from bench to bedside. Eur. Heart J. *36*, 3404–3412.

Xiong, J., Kawagishi, H., Yan, Y., Liu, J., Wells, Q.S., Edmunds, L.R., Fergusson, M.M., Yu, Z.X., Rovira, I.I., Brittain, E.L., et al. (2018). A metabolic basis for endothelial-to-mesenchymal transition. Mol. Cell *69*, 689–698.e7.

Xu, J., Eilat-Adar, S., Loria, C., Goldbourt, U., Howard, B.V., Fabsitz, R.R., Zephier, E.M., Mattil, C., and Lee, E.T. (2006). Dietary fat intake and risk of coronary heart disease: the Strong Heart Study. Am. J. Clin. Nutr *84*, 894–902.

Xu, Z.J., Fan, J.G., Ding, X.D., Qiao, L., and Wang, G.L. (2010). Characterization of high-fat, diet-induced, non-alcoholic steatohepatitis with fibrosis in rats. Dig. Dis. Sci. *55*, 931–940.

Yanagisawa, N., Shimada, K., Miyazaki, T., Kume, A., Kitamura, Y., Sumiyoshi, K., Kiyanagi, T., Iesaki, T., Inoue, N., and Daida, H. (2008). Enhanced production of nitric oxide, reactive oxygen species, and pro-inflammatory cytokines in very long chain saturated fatty acid-accumulated macrophages. Lipids Health Dis. *7*, 48.

Yang, W., Nagasawa, K., Münch, C., Xu, Y., Satterstrom, K., Jeong, S., Hayes, S.D., Jedrychowski, M.P., Vyas, F.S., Zaganjor, E., et al. (2016). Mitochondrial sirtuin network reveals dynamic SIRT3-dependent deacetylation in response to membrane depolarization. Cell *167*, 985–1000.e21.

Yore, M.M., Syed, I., Moraes-Vieira, P.M., Zhang, T., Herman, M.A., Homan, E.A., Patel, R.T., Lee, J., Chen, S., Peroni, O.D., et al. (2014). Discovery of a class of endogenous mammalian lipids with anti-diabetic and anti-inflammatory effects. Cell *159*, 318–332.

Yu, W., Dittenhafer-Reed, K.E., and Denu, J.M. (2012). SIRT3 protein deacetylates isocitrate dehydrogenase 2 (IDH2) and regulates mitochondrial redox status. J. Biol. Chem. *287*, 14078–14086.

Zhu, Y., Zou, X., Dean, A.E., Brien, J.O., Gao, Y., Tran, E.L., Park, S.H., Liu, G., Kieffer, M.B., Jiang, H., et al. (2019). Lysine 68 acetylation directs MnSOD as a tetrameric detoxification complex versus a monomeric tumor promoter. Nat. Commun. *10*, 2399.